

## Parabolic approximation, radiative transfer and time reversal

This article has been downloaded from IOPscience. Please scroll down to see the full text article.

2005 J. Phys.: Conf. Ser. 7 121

(<http://iopscience.iop.org/1742-6596/7/1/010>)

View [the table of contents for this issue](#), or go to the [journal homepage](#) for more

### Download details:

IP Address: 169.237.215.179

The article was downloaded on 14/05/2010 at 20:07

Please note that [terms and conditions apply](#).

# Parabolic Approximation, Radiative Transfer and Time Reversal

**Albert C. Fannjiang**

Department of Mathematics, University of California at Davis, Davis, CA 95616

E-mail: [cafannjiang@ucdavis.edu](mailto:cafannjiang@ucdavis.edu)

**Abstract.** We first present a new formulation of parabolic approximation of the Maxwell equations for heterogeneous dielectric materials. We then discuss rigorous results about self-averaging scaling limits of parabolic waves in terms of the Wigner distribution function. Among the 6 possible scaling limits two are exactly solvable. We use the Green function to analyze the time-reversed operation in turbulent media with power-law spectral density. We show that the time-reversed refocused spot size depends superlinearly on the wavelength and thus has the potential of breaking the diffraction limit when the wavelength is small.

We also derive an uncertainty principle for random media which has the forward wave spread and the turbulence-induced resolution as conjugate quantities.

## 1. Introduction

Wave propagation in random media is an important problem for both fundamental and practical reasons.

In the fundamental aspect, randomness often introduces completely new phenomena into the physical processes. One such example is the localization of the Schrödinger wave in a strongly fluctuating random medium. A related effect is the enhanced backscattering of waves in random media. Another example is the transition of the Bloch waves in a periodic medium to the diffusive wave regime when random impurities are added to the medium. In the practical aspect, randomness is often viewed as impedance to various technologies such as distortion of wave fronts and astronomical images for ground-based telescopes. Adaptive optics and space telescopes (such as the Hubble Space Telescope) were invented to circumvent the difficulties caused by the atmospheric turbulence. In satellite or wireless communications the multi-path effect of a random medium causes the inter-symbol-interference which induces errors in communication or slows down the rate of transmission.

Unfortunately the full governing equations describing wave processes in random media are often extremely challenging to solve even for computers. It is thus very important to identify asymptotic regimes where simplified description can be effective and to devise efficient numerical schemes for computer simulation.

In the present paper, we first review the vector wave equations for electro-magnetic waves in dielectric materials. Then we present a novel iterative scheme which has demonstrable advantages. Next we discuss a family of self-averaging scaling limits, including the radiative transfer limit, which arise when the correlation length of the medium fluctuation is relatively

short and the intensity of the fluctuation is relatively large. Finally we use the Green function of one of the exactly solvable limits to analyze the time reversal of waves in random media.

Time reversal of waves has been a hot topic because many new possibilities have been demonstrated experimentally in laboratories and nature environments (mostly with the sound waves) [3, 6, 4, 5, 11, 12, 13, 14, 17, ?, 22, 24, 26]. An interesting effect of time reversal operation with random media is the statistical stability of the refocal spot, independent of the medium realization from the same ensemble, when the time-reversal aperture is large compared to the correlation length of the medium fluctuations. This statistical stability or self-averaging effect is partially but rigorously addressed by one of our self-averaging scaling regimes. Another regime of statistical stability not addressed in this paper is the use of broadband signals. The most striking effect in time-reversed back-propagated waves in random media is that the refocused spot size can be much *smaller* than that in the homogeneous medium. Here the random medium appears as *enhancement*, instead of impedance, to the resolution. This is called superresolution which in a particular regime has already been explained by using a radiative transfer equation in [2]. In the previous experimental, numerical or theoretical results the superresolution comes as a *linear* function of the wavelength but independent of the aperture. We show that in fractal media the resolution can be a *superlinear* (between linear and quadratic) function of the wavelength. The lowest achievable refocal spot size in this nonlinear regime is on the order of the smallest scale of the medium fluctuations. Below this scale the linear regime prevails.

Finally we derive an uncertainty principle for random media which has the forward wave spread and the turbulence-induced resolution as conjugate quantities.

## 2. Maxwell equations for dielectric materials

Let us start with the Maxwell equations for a dielectric medium where there is no free charges  $\rho = 0$  and no current flows  $\mathbf{j} = 0$  and the only material response is the induced dipole polarization  $\mathbf{P}$ :

$$\nabla \times \mathbf{E} = -\frac{\partial}{\partial t} \mathbf{B} \quad (1)$$

$$\nabla \times \mathbf{H} = \frac{\partial}{\partial t} \mathbf{D} \quad (2)$$

$$\nabla \cdot \mathbf{D} = 0 \quad (3)$$

$$\nabla \cdot \mathbf{B} = 0. \quad (4)$$

Here  $\mathbf{E}$  and  $\mathbf{D}$  are, respectively, the electric field and the displacement field, and are related by

$$\mathbf{D} = \epsilon_0 \mathbf{E} + \mathbf{P} = \epsilon \mathbf{E} \quad (5)$$

with the dielectric constants  $\epsilon_0$  (of the vacuum) and  $\epsilon$  (of the dielectric material);  $\mathbf{H}$  and  $\mathbf{B}$  are, respectively, the magnetic field and the magnetic induction and are related by

$$\mathbf{B} = \mu \mathbf{H} \quad (6)$$

with the magnetic permeability  $\mu$  of the medium. The magnetic permeability of the vacuum is denoted by  $\mu_0$ . Eq. (1) and (2) are the dynamical equations; eq. (3) and (4) are the constraints; eq. (5) and (6) are the constitutive equations. We note that para- and diamagnetisms are always very weak, so that for non-ferromagnetic materials it is essentially true that  $\mu = \mu_0$ . For ferromagnetic materials,  $\mu$  is also essentially equal to  $\mu_0$  in the optical range of frequency  $\omega$  since ferromagnetism does not occur at high frequencies.

The local speed of propagation  $c(\vec{\mathbf{x}})$ ,  $\vec{\mathbf{x}} \in \mathbb{R}^3$  is given by

$$c = \frac{1}{\sqrt{\epsilon\mu}} = \frac{c_0}{n}$$

where  $n(\vec{\mathbf{x}})$  is the refractive index field at  $\vec{\mathbf{x}}$  given by

$$n(\vec{\mathbf{x}}) = \sqrt{\frac{\epsilon}{\epsilon_0}}.$$

Taking the curl of eq. (1) and using eq. (2), (5) we obtain

$$\Delta \mathbf{E} - \nabla(\nabla \cdot \mathbf{E}) = c^{-2} \frac{\partial^2}{\partial t^2} \mathbf{E}. \quad (7)$$

Using the constitutive relation (5) and the constraint (3) the second term on the LHS can be expressed as

$$\nabla \cdot \mathbf{E} = \nabla \cdot \frac{\mathbf{D}}{\epsilon} = -\epsilon^{-2} \nabla \epsilon \cdot \mathbf{D} = -\epsilon^{-1} \nabla \epsilon \cdot \mathbf{E}. \quad (8)$$

With this we arrive at the wave equation

$$\Delta \mathbf{E} + \nabla (\epsilon^{-1} \nabla \epsilon \cdot \mathbf{E}) = c_0^{-2} \epsilon_0^{-1} \epsilon(\mathbf{x}) \frac{\partial^2}{\partial t^2} \mathbf{E} \quad (9)$$

or in terms of the refractive index

$$\Delta \mathbf{E} + 2\nabla (n^{-1} \nabla n \cdot \mathbf{E}) = c_0^{-2} n^2 \frac{\partial^2}{\partial t^2} \mathbf{E}. \quad (10)$$

Let us write the electric susceptibility  $\chi = \epsilon/\epsilon_0$  as

$$\chi = \bar{\chi}(1 + \tilde{\chi}(\vec{\mathbf{x}})), \quad \vec{\mathbf{x}} \in \mathbb{R}^3$$

where  $\bar{\chi}$  is the background (relative) dielectric constant and  $\tilde{\chi}$  the fluctuation. Taking the Fourier transform in time we obtain from eq. (9) that

$$\Delta \hat{\mathbf{E}} + \nabla \left( (1 + \tilde{\chi})^{-1} \nabla \tilde{\chi} \cdot \hat{\mathbf{E}} \right) + k^2 \bar{\chi} (1 + \tilde{\chi}) \hat{\mathbf{E}} = 0 \quad (11)$$

where

$$k = \omega/c_0$$

is the wavenumber in vacuum.

### 3. Coupled forward-backward equations with polarization

Let us consider the high frequency wave  $k \gg 1$ . We assume that the waves propagate primarily in the  $z$  direction and we write  $\vec{\mathbf{x}} = (z, \mathbf{x})$  where  $\mathbf{x}$  is the coordinates in the transverse directions.

Following [18] we consider the following ansatz

$$\hat{\mathbf{E}} = \mathbf{A} e^{i\sqrt{\bar{\chi}}kz} + \mathbf{B} e^{-i\sqrt{\bar{\chi}}kz}. \quad (12)$$

We can interpret  $\mathbf{A}$  and  $\mathbf{B}$  as the forward and backward propagating modes, respectively.

Differentiating with respect to  $z$  we have

$$\hat{\mathbf{E}}_z = \mathbf{A}_z e^{i\sqrt{\bar{\chi}}kz} + \mathbf{B}_z e^{-i\sqrt{\bar{\chi}}kz} + i\sqrt{\bar{\chi}}k \left( \mathbf{A} e^{i\sqrt{\bar{\chi}}kz} - \mathbf{B} e^{-i\sqrt{\bar{\chi}}kz} \right). \quad (13)$$

For high frequency waves  $k \gg 1$  we now make the following approximation

$$\hat{\mathbf{E}}_z = i\sqrt{\bar{\chi}}k \left( \mathbf{A} e^{i\bar{\chi}kz} - \mathbf{B} e^{-i\bar{\chi}kz} \right) \quad (14)$$

or equivalently

$$\mathbf{A}_z e^{i\sqrt{\tilde{\chi}}kz} + \mathbf{B}_z e^{-i\sqrt{\tilde{\chi}}kz} = 0. \quad (15)$$

Differentiating eq. (15) w.r.t.  $z$  again and using (15) we obtain

$$\left( \mathbf{A}_{zz} e^{i\sqrt{\tilde{\chi}}kz} + \mathbf{B}_{zz} e^{-i\sqrt{\tilde{\chi}}kz} \right) = i2k\sqrt{\tilde{\chi}}\mathbf{B}_z e^{-i\sqrt{\tilde{\chi}}kz} \quad (16)$$

and

$$\left( \mathbf{A}_{zz} e^{i\sqrt{\tilde{\chi}}kz} + \mathbf{B}_{zz} e^{-i\sqrt{\tilde{\chi}}kz} \right) = -i2k\sqrt{\tilde{\chi}}\mathbf{A}_z e^{i\sqrt{\tilde{\chi}}kz} \quad (17)$$

which will be used later.

Substituting (12) into eq. (11) and canceling the background propagation components we get

$$\begin{aligned} & e^{i\sqrt{\tilde{\chi}}kz} \left[ \Delta_{\perp} \mathbf{A} + \mathbf{A}_{zz} + i2\sqrt{\tilde{\chi}}k\mathbf{A}_z + k^2\tilde{\chi}\tilde{\chi}\mathbf{A} + \mathbf{A}_z(1+\tilde{\chi})^{-1}\tilde{\chi}_z \right. \\ & \left. + \nabla_{\perp} \mathbf{A} \cdot \left( (1+\tilde{\chi})^{-1}\nabla_{\perp}\tilde{\chi} \right) + i\sqrt{\tilde{\chi}}k(1+\tilde{\chi})^{-1}(\nabla\tilde{\chi} \cdot \mathbf{A})\mathbf{e}_z + (\nabla(1+\tilde{\chi})^{-1}\nabla\tilde{\chi}) \cdot \mathbf{A} \right] \\ = & e^{-i\sqrt{\tilde{\chi}}kz} \left[ -\Delta_{\perp} \mathbf{B} - \mathbf{B}_{zz} + i2\sqrt{\tilde{\chi}}k\mathbf{B}_z - k^2\tilde{\chi}\tilde{\chi}\mathbf{B} - \mathbf{B}_z(1+\tilde{\chi})^{-1}\tilde{\chi}_z \right. \\ & \left. - \nabla_{\perp} \mathbf{B} \cdot \left( (1+\tilde{\chi})^{-1}\nabla_{\perp}\tilde{\chi} \right) + i\sqrt{\tilde{\chi}}k(1+\tilde{\chi})^{-1}(\nabla\tilde{\chi} \cdot \mathbf{B})\mathbf{e}_z - (\nabla(1+\tilde{\chi})^{-1}\nabla\tilde{\chi}) \cdot \mathbf{B} \right]. \end{aligned} \quad (18)$$

Now by (16) and (15) eq. (18) reduces to

$$\begin{aligned} & i2\sqrt{\tilde{\chi}}k\mathbf{A}_z + \Delta_{\perp} \mathbf{A} + k^2\tilde{\chi}\tilde{\chi}\mathbf{A} \\ & + \nabla_{\perp} \mathbf{A} \cdot \left( (1+\tilde{\chi})^{-1}\nabla_{\perp}\tilde{\chi} \right) + i\sqrt{\tilde{\chi}}k(1+\tilde{\chi})^{-1}(\nabla\tilde{\chi} \cdot \mathbf{A})\mathbf{e}_z + (\nabla(1+\tilde{\chi})^{-1}\nabla\tilde{\chi}) \cdot \mathbf{A} \\ = & e^{-i2\sqrt{\tilde{\chi}}kz} \left[ -\Delta_{\perp} \mathbf{B} - k^2\tilde{\chi}\tilde{\chi}\mathbf{B} \right. \\ & \left. - \nabla_{\perp} \mathbf{B} \cdot \left( (1+\tilde{\chi})^{-1}\nabla_{\perp}\tilde{\chi} \right) + i\sqrt{\tilde{\chi}}k(1+\tilde{\chi})^{-1}(\nabla\tilde{\chi} \cdot \mathbf{B})\mathbf{e}_z - (\nabla(1+\tilde{\chi})^{-1}\nabla\tilde{\chi}) \cdot \mathbf{B} \right]. \end{aligned} \quad (19)$$

On the other hand, by (15) and (17) eq. (18) reduces instead to

$$\begin{aligned} & -i2\sqrt{\tilde{\chi}}k\mathbf{B}_z + \Delta_{\perp} \mathbf{B} + k^2\tilde{\chi}\tilde{\chi}\mathbf{B} \\ & + \nabla_{\perp} \mathbf{B} \cdot \left( (1+\tilde{\chi})^{-1}\nabla_{\perp}\tilde{\chi} \right) - i\sqrt{\tilde{\chi}}k(1+\tilde{\chi})^{-1}(\nabla\tilde{\chi} \cdot \mathbf{B})\mathbf{e}_z + (\nabla(1+\tilde{\chi})^{-1}\nabla\tilde{\chi}) \cdot \mathbf{B} \\ = & e^{i2\sqrt{\tilde{\chi}}kz} \left[ -\Delta_{\perp} \mathbf{A} - k^2\tilde{\chi}\tilde{\chi}\mathbf{A} \right. \\ & \left. - \nabla_{\perp} \mathbf{A} \cdot \left( (1+\tilde{\chi})^{-1}\nabla_{\perp}\tilde{\chi} \right) - i\sqrt{\tilde{\chi}}k(1+\tilde{\chi})^{-1}(\nabla\tilde{\chi} \cdot \mathbf{A})\mathbf{e}_z - (\nabla(1+\tilde{\chi})^{-1}\nabla\tilde{\chi}) \cdot \mathbf{A} \right]. \end{aligned} \quad (20)$$

Here  $\nabla_{\perp} = \nabla_{\mathbf{x}}$  is the transverse gradient and  $\Delta_{\perp} = \Delta_{\mathbf{x}}$  is the transverse Laplacian. The main feature in the above system is that  $z$ -derivative of  $\mathbf{A}$  or  $\mathbf{B}$  is first order and appears only once in either equation. We note that the above procedure is exact including the relation (15) which can be viewed as a constraint to eliminate the redundancy in the ansatz (12).

The coupled forward and backward modes (19), (20) take the following form

$$i2\sqrt{\tilde{\chi}}k\frac{\partial}{\partial z}\mathbf{A} + \mathcal{L}_1\mathbf{A} = -e^{-i2\sqrt{\tilde{\chi}}kz}\mathcal{L}_2\mathbf{B} \quad (21)$$

$$-i2\sqrt{\tilde{\chi}}k\frac{\partial}{\partial z}\mathbf{B} + \mathcal{L}_2\mathbf{B} = -e^{i2\sqrt{\tilde{\chi}}kz}\mathcal{L}_1\mathbf{A} \quad (22)$$

where the operators  $\mathcal{L}_1$  and  $\mathcal{L}_2$  given by

$$\begin{aligned} \mathcal{L}_1\mathbf{A} = & \Delta_{\perp} \mathbf{A} + k^2\tilde{\chi}\tilde{\chi}\mathbf{A} \\ & + \nabla_{\perp} \mathbf{A} \cdot \left( (1+\tilde{\chi})^{-1}\nabla_{\perp}\tilde{\chi} \right) + i\sqrt{\tilde{\chi}}k(1+\tilde{\chi})^{-1}(\nabla\tilde{\chi} \cdot \mathbf{A})\mathbf{e}_z + (\nabla(1+\tilde{\chi})^{-1}\nabla\tilde{\chi}) \cdot \mathbf{A} \end{aligned} \quad (23)$$

$$\begin{aligned} \mathcal{L}_2\mathbf{B} = & \Delta_{\perp} \mathbf{B} + k^2\tilde{\chi}\tilde{\chi}\mathbf{B} \\ & + \nabla_{\perp} \mathbf{B} \cdot \left( (1+\tilde{\chi})^{-1}\nabla_{\perp}\tilde{\chi} \right) - i\sqrt{\tilde{\chi}}k(1+\tilde{\chi})^{-1}(\nabla\tilde{\chi} \cdot \mathbf{B})\mathbf{e}_z + (\nabla(1+\tilde{\chi})^{-1}\nabla\tilde{\chi}) \cdot \mathbf{B} \end{aligned} \quad (24)$$

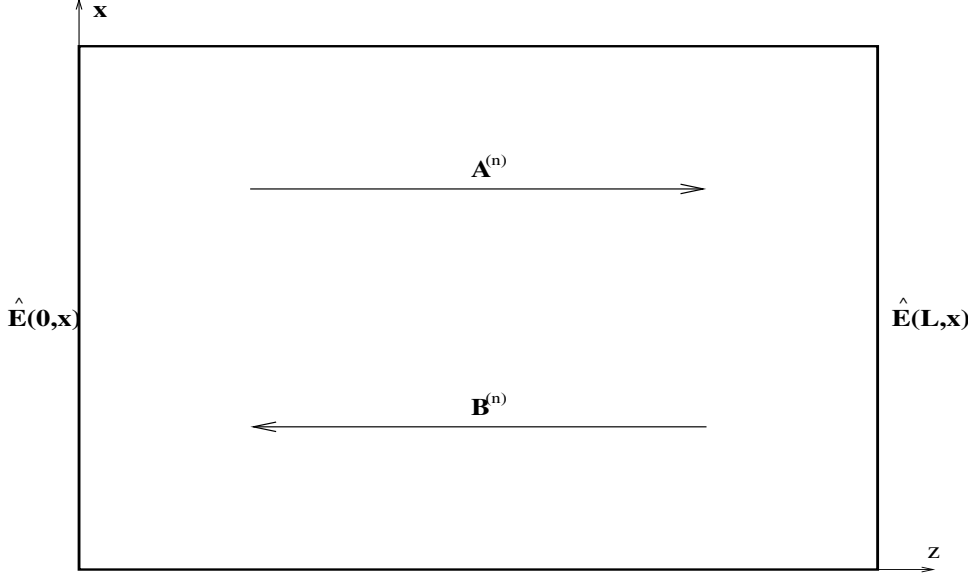


**Figure 1.** Iteration scheme for solving the wave equation

involve only the transverse differentiation. The main advantage of formulating the reduced wave equation in the form (11) is that the original boundary value problem associated with (11) can be solved iteratively from  $z = 0$  to  $z = L$  by solving eq. (21) and then from  $z = L$  to  $z = 0$  by solving eq. (22):

$$\begin{aligned} i2\sqrt{\chi}k \frac{\partial}{\partial z} \mathbf{A}^{(n)} + \mathcal{L}_1 \mathbf{A}^{(n)} &= -e^{-i2\sqrt{\chi}kz} \mathcal{L}_2 \mathbf{B}^{(n-1)}, & \mathbf{A}^{(n)}(0, \mathbf{x}) &= \hat{\mathbf{E}}(0, \mathbf{x}) - \mathbf{B}^{(n-1)}(0, \mathbf{x}) \\ -i2\sqrt{\chi}k \frac{\partial}{\partial z} \mathbf{B}^{(n)} + \mathcal{L}_2 \mathbf{B}^{(n)} &= -e^{i2\sqrt{\chi}kz} \mathcal{L}_1 \mathbf{A}^{(n)}, & \mathbf{B}^{(n)}(L, \mathbf{x}) &= e^{i\sqrt{\chi}kL} \hat{\mathbf{E}}(L, \mathbf{x}) - e^{i2\sqrt{\chi}kL} \mathbf{A}^{(n)} \end{aligned} \quad (25)$$

for  $n = 1, 2, 3, \dots$  with  $\mathbf{B}^{(0)} = 0$ . The computational cost can be significantly lowered than the direct solver of eq. (11). For simplicity, we assume that the transverse cross section of the domain is a rectangle with widths  $L_x, L_y$  and we assume either the zero or periodic boundary condition.

### 3.1. Hierarchy of approximations

In the weak scattering regime  $k \gg |\chi^{-1} \nabla \chi|$ , the leading order approximation to the system (19)-(20) is the system of parabolic wave equations

$$i2\sqrt{\chi}k \mathbf{A}_z + \Delta_{\perp} \mathbf{A} + k^2 \bar{\chi} \tilde{\chi} \mathbf{A} = 0 \quad (27)$$

$$-i2\sqrt{\chi}k \mathbf{B}_z + \Delta_{\perp} \mathbf{B} + k^2 \bar{\chi} \tilde{\chi} \mathbf{B} = 0. \quad (28)$$

The terms

$$e^{-i2\sqrt{\chi}kz} k^2 \bar{\chi} \tilde{\chi} \mathbf{B}, \quad e^{-i2\sqrt{\chi}kz} k^2 \bar{\chi} \tilde{\chi} \mathbf{A}$$

can be neglected for fast phase if  $kL \gg 1$  in the case of the transport or diffusive regime. Equation-wise, this is the standard parabolic (or paraxial) approximation which is widely used for waves in weakly fluctuating refractive index fields (see for example [19]). However, (27) and (28) are still coupled through the boundary conditions as in (25)-(26). Only the different polarizations are decoupled.

The next order approximation is to include the term of the order  $k^2$  on the RHS of the system. The resulting equations are the coupled system of the forward and backward modes:

$$i2\sqrt{\bar{\chi}}k\mathbf{A}_z + \Delta_{\perp}\mathbf{A} + k^2\bar{\chi}\tilde{\chi}\mathbf{A} = -e^{-i2\sqrt{\bar{\chi}}kz}k^2\bar{\chi}\tilde{\chi}\mathbf{B} \quad (29)$$

$$-i2\sqrt{\bar{\chi}}k\mathbf{B}_z + \Delta_{\perp}\mathbf{B} + k^2\bar{\chi}\tilde{\chi}\mathbf{B} = -e^{i2\sqrt{\bar{\chi}}kz}k^2\bar{\chi}\tilde{\chi}\mathbf{A}. \quad (30)$$

This coupled system has been numerically demonstrated to yield solutions more closely approximating those of the reduced wave equation (11) than the decoupled system (27)-(28) especially in the small scale behavior [18]. As in the system (27)-(28) the different polarizations are decoupled in (29)-(29).

Let  $L_0$  be the correlation length of  $\tilde{\chi}$ . When  $\tilde{\chi}$  is highly fluctuating as in the case of long distance propagation  $L \gg L_0$  or in the case of wide beam width  $L_{\perp} \gg L_0$ , it is no longer reasonable to discard entirely the second lines on the LHS of (19)-(20). Namely, the different components of the wave are coupled due to inhomogeneities.

We write explicitly the transverse and longitudinal components as  $\mathbf{A} = (\mathbf{A}^{\perp}, A')$ ,  $\mathbf{B} = (\mathbf{B}^{\perp}, B')$ . We assume still the high frequency regime  $kL_0 \gg 1$ . Then the equations for the transverse modes satisfy

$$i2\sqrt{\bar{\chi}}k\mathbf{A}_z^{\perp} + \Delta_{\perp}\mathbf{A}^{\perp} + k^2\bar{\chi}\tilde{\chi}\mathbf{A}^{\perp} + [(\nabla(1 + \tilde{\chi})^{-1}\nabla\tilde{\chi}) \cdot \mathbf{A}]^{\perp} = -e^{-i2\sqrt{\bar{\chi}}kz}k^2\bar{\chi}\tilde{\chi}\mathbf{B}^{\perp} \quad (31)$$

$$-i2\sqrt{\bar{\chi}}k\mathbf{B}_z^{\perp} + \Delta_{\perp}\mathbf{B}^{\perp} + k^2\bar{\chi}\tilde{\chi}\mathbf{B}^{\perp} + [(\nabla(1 + \tilde{\chi})^{-1}\nabla\tilde{\chi}) \cdot \mathbf{B}]^{\perp} = -e^{i2\sqrt{\bar{\chi}}kz}k^2\bar{\chi}\tilde{\chi}\mathbf{A}^{\perp} \quad (32)$$

while the longitudinal modes satisfy

$$i2\sqrt{\bar{\chi}}kA'_z + \Delta_{\perp}A' + k^2\bar{\chi}\tilde{\chi}A' + i\sqrt{\bar{\chi}}k(1 + \tilde{\chi})^{-1}\nabla\tilde{\chi} \cdot \mathbf{A} = -e^{-i2\sqrt{\bar{\chi}}kz}k^2\bar{\chi}\tilde{\chi}B' \quad (33)$$

$$-i2\sqrt{\bar{\chi}}kB'_z + \Delta_{\perp}B' + k^2\bar{\chi}\tilde{\chi}B' - i\sqrt{\bar{\chi}}k(1 + \tilde{\chi})^{-1}\nabla\tilde{\chi} \cdot \mathbf{B} = -e^{i2\sqrt{\bar{\chi}}kz}k^2\bar{\chi}\tilde{\chi}A'. \quad (34)$$

The rest of the paper, however, will focus on the analysis of the parabolic system (27)-(28) as the analysis of the other two systems are much more complicated and still work in progress.

### 3.2. Decomposition of the data

Let us first consider the homogeneous case where  $\bar{\chi} = 1$  and  $\tilde{\chi} = 0$ . Let  $U_z$  be the corresponding propagator such that

$$U_z f(\mathbf{x}) = \frac{k}{2\pi z} \int \exp\left[-i\frac{k}{2z}|\mathbf{x} - \mathbf{y}|^2\right] f(\mathbf{y}) d\mathbf{y}.$$

Then we have the expression for  $\mathbf{A}^{(n+1)}$

$$\mathbf{A}^{(n+1)}(0, \mathbf{x}) = \sum_{m=0}^n e^{i2mkL} U_L^{2m} \hat{\mathbf{E}}(0, \mathbf{x}) - e^{ikL} U_L \sum_{m=0}^{n-1} e^{i2mkL} U_L^{2m} \hat{\mathbf{E}}(L, \mathbf{x}). \quad (35)$$

If the limits  $\mathbf{A}^{\infty}(0, \mathbf{x}) \equiv \lim_{n \rightarrow \infty} \mathbf{A}^{(n)}(0, \mathbf{x})$ ,  $\mathbf{B}^{\infty}(L, \mathbf{x}) \equiv \lim_{n \rightarrow \infty} \mathbf{B}^{(n)}(L, \mathbf{x})$  exist then they satisfy the equations

$$\left(1 - e^{2ikL} U_L^2\right) \mathbf{A}^{\infty}(0, \mathbf{x}) = \mathbf{E}(0, \mathbf{x}) - e^{ikL} U_L \mathbf{E}(L, \mathbf{x}) \quad (36)$$

$$\left(1 - e^{2ikL} U_L^2\right) \mathbf{B}^{\infty}(L, \mathbf{x}) = e^{ikL} \mathbf{E}(L, \mathbf{x}) - e^{i2kL} U_L \mathbf{E}(0, \mathbf{x}). \quad (37)$$

Let  $\beta$  be the bandwidth of the boundary data  $\hat{\mathbf{E}}(0, \mathbf{x})$ ,  $\hat{\mathbf{E}}(L, \mathbf{x})$ . For

$$\beta < \sqrt{2}k \quad (38)$$

the RHS of eq. (36) and (37) are orthogonal to the null space of the adjoint of  $1 - e^{i2kL}U_L^2$ , denoted by  $\ker(1 - e^{i2kL}U_L^2)^*$ , and hence eq. (36) and (37) have a unique solution in the orthogonal complement of  $\ker(1 - e^{i2kL}U_L^2)^*$ . The solutions are such that

$$e^{ikL}U_L\mathbf{A}^\infty(0, \mathbf{x}) + e^{-ikL}\mathbf{B}^\infty(L, \mathbf{x}) = \mathbf{E}(L, \mathbf{x}) \quad (39)$$

$$U_L\mathbf{B}^\infty(L, \mathbf{x}) + \mathbf{A}(0, \mathbf{x}) = \mathbf{E}(0, \mathbf{x}). \quad (40)$$

With the boundary data decomposed in the following way

$$\hat{\mathbf{E}}(0, \mathbf{x}) = \mathbf{A}^\infty(0, \mathbf{x}) + \mathbf{B}^\infty(0, \mathbf{x}), \quad \mathbf{B}^\infty(0, \mathbf{x}) = \left(\hat{\mathbf{E}}(0, \mathbf{x}) - \mathbf{A}^\infty(0, \mathbf{x})\right)$$

$$\hat{\mathbf{E}}(L, \mathbf{x}) = \mathbf{A}^\infty(L, \mathbf{x})e^{ikL} + \mathbf{B}^\infty(L, \mathbf{x})e^{-ikL}, \quad \mathbf{A}^\infty(L, \mathbf{x}) = e^{-ikL} \left(\hat{\mathbf{E}}(L, \mathbf{x}) - \mathbf{B}^\infty(L, \mathbf{x})e^{-ikL}\right)$$

eq. (27) and (28) completely decouple from each other.

In the presence of an inhomogeneous electric susceptibility  $\tilde{\chi}$ , the problem of decomposing the data can be reduced to studying the wellposedness of the equations

$$\left(1 - e^{2ikL}\tilde{U}_L U_L\right) \mathbf{A}^\infty(0, \mathbf{x}) = \mathbf{E}(0, \mathbf{x}) - e^{ikL}\tilde{U}_L \mathbf{E}(L, \mathbf{x}) \quad (41)$$

$$\left(1 - e^{2ikL}U_L \tilde{U}_L\right) \mathbf{B}^\infty(L, \mathbf{x}) = e^{ikL}\mathbf{E}(L, \mathbf{x}) - e^{i2kL}U_L \mathbf{E}(0, \mathbf{x}) \quad (42)$$

where  $U_L$  and  $\tilde{U}_L$  are the (random) propagator associated with the one-sweep random Schrödinger equations (27) and (28) respectively. The null space of the operator adjoint to the LHS of (41)-(42) is not easy to characterize in general. However, the system (41)-(42) is well-posed provided that  $\exp(-i2Lk)$  is not in the spectrum of the unitary operator  $\tilde{U}_L U_L$  or  $U_L \tilde{U}_L$ .

In the following we will focus on the self-averaging regimes where a quadratic functional of the wave amplitude, called the Wigner distribution, has a deterministic limit which is very important in the time-reversal analysis discussed in Section 5. Because different polarizations are decoupled in (27)-(28) we will use the scalar version of (27) and denote the amplitude by  $\Psi$ .

#### 4. Self-averaging scaling limits

Next we present an overview of some recently proved scaling limits for high-frequency wave transport in random media using the phase space formulation, called the Wigner distribution. We then solve exactly two solvable limiting models and apply the results to time reversal of waves.

Let us nondimensionalize the equation by two reference scales of observation  $L_z = L$  for the longitudinal coordinate and  $L_x = L_y$  for the transverse coordinates, and the reference frequency  $k_0$ . Introducing the rescaled quantities

$$\tilde{\mathbf{x}} = \mathbf{x}/L_x, \quad \tilde{z} = z/L_z, \quad \tilde{k} = k/k_0$$

and dropping the tilde in  $\tilde{z}, \tilde{\mathbf{x}}$  after rescaling we obtain the parabolic equation in the rescaled variables

$$i\frac{\partial}{\partial z}\Psi(z, \mathbf{x}) + \frac{\gamma}{2\tilde{k}}\nabla^2\Psi(z, \mathbf{x}) + \frac{k_0}{2}\tilde{k}L_z\tilde{\chi}(zL_z, \mathbf{x}L_x)\Psi(z, \mathbf{x}) = 0. \quad (43)$$

where  $\gamma$  is the dimensionless Fresnel number

$$\gamma = \frac{L_z}{k_0\bar{\chi}L_x^2}.$$

Let us write

$$\tilde{\chi}(zL_z, \mathbf{x}L_x) = \kappa V(z\ell_z, \mathbf{x}\ell_x),$$

with

$$\ell_z = \frac{L_z}{L_0}, \quad \ell_x = \frac{L_x}{L_0}$$

where  $\kappa$  is the standard variation of the statistically homogeneous field  $\tilde{\chi}(z, \mathbf{x})$  and  $L_0$  is the correlation length of the index fluctuation so that  $V$  is the normalized electric susceptibility field with  $O(1)$  correlation length. We then rewrite (43) as

$$i\frac{\partial\Psi}{\partial z} + \frac{\gamma}{2k}\Delta\Psi + \tilde{k}\sigma V(z\ell_z, \mathbf{x}\ell_x)\Psi = 0 \quad (44)$$

with the dimensionless parameters

$$\sigma = k_0 L_z \bar{\chi} \kappa / 2. \quad (45)$$

The self-averaging scalings are to let  $\ell_z, \ell_x, \sigma \rightarrow \infty$  and  $\gamma \rightarrow 0$  in various controlled ways.

Since the self-averaging limits require  $\ell_x \rightarrow \infty$  we shall assume for simplicity that the physical domain is an infinite slab unbounded in the transverse dimensions. The effective size of the domain, however, is determined by the boundary data and remains  $O(1)$ .

#### 4.1. Assumptions on the electric susceptibility

We assume that  $V(z, \mathbf{x})$  is a centered,  $z$ -stationary,  $\mathbf{x}$ -homogeneous random field admitting the spectral representation

$$V(z, \mathbf{x}) = \int \exp(i\mathbf{p} \cdot \mathbf{x}) \hat{V}(z, d\mathbf{p})$$

with the  $z$ -stationary spectral measure  $\hat{V}(z, \cdot)$  satisfying

$$\mathbb{E}[\hat{V}(z, d\mathbf{p})\hat{V}(z, d\mathbf{q})] = \delta(\mathbf{p} + \mathbf{q})\Phi_0(\mathbf{p})d\mathbf{p}d\mathbf{q}.$$

The transverse power spectrum density is related to the full power spectrum density  $\Phi(\xi, \mathbf{p})$  in the following way

$$\Phi_0(\mathbf{p}) = \int \Phi(\xi, \mathbf{p})d\xi.$$

The power spectral density  $\Phi(\vec{\mathbf{k}})$  satisfies  $\Phi(\vec{\mathbf{k}}) = \Phi(-\vec{\mathbf{k}})$ ,  $\forall \vec{\mathbf{k}} = (\xi, \mathbf{p}) \in \mathbb{R}^{d+1}$  because the electric susceptibility field is assumed to be real-valued. Hence

$$\Phi(w, \mathbf{p}) = \Phi(-w, \mathbf{p}) = \Phi(w, -\mathbf{p}) = \Phi(-w, -\mathbf{p}) \quad (46)$$

which is related to the detailed balance of the limiting scattering operators described below.

**Assumption 1**  $V_z(\mathbf{x})$  is a square-integrable,  $z$ -stationary,  $\mathbf{x}$ -homogeneous Gaussian process with a spectral density satisfying the upper bound

$$\Phi(\vec{\mathbf{k}}) \leq K(\ell_1^{-2} + |\vec{\mathbf{k}}|^2)^{-H-1/2-d/2} \left(1 + \ell_0^2 |\vec{\mathbf{k}}|^2\right)^{-2}, \quad \vec{\mathbf{k}} \in \mathbb{R}^{d+1}, \quad H \in (0, 1) \quad (47)$$

for some positive constants  $K, \ell_0, \ell_1$ .

A relevant example is the generalized von Kármán spectral density with  $H = 1/3$  [19].

Let  $\mathcal{F}_z$  and  $\mathcal{F}_z^+$  be the sigma-algebras generated by  $\{V_s : \forall s \leq z\}$  and  $\{V_s : \forall s \geq z\}$ , respectively. The correlation coefficient  $r(t)$  is given by

$$r(t) = \sup_{\substack{h \in \mathcal{F}_z \\ \mathbb{E}[h]=0, \mathbb{E}[h^2]=1}} \sup_{\substack{g \in \mathcal{F}_{z+t}^+ \\ \mathbb{E}[g]=0, \mathbb{E}[g^2]=1}} \mathbb{E}[hg]. \quad (48)$$

We assume

**Assumption 2** *The correlation coefficient  $r(t)$  satisfies*

$$\int_0^\infty r(s) ds < \infty.$$

#### 4.2. Radiative transfer equations

First we consider a family of scaling limits with

$$\gamma \ll 1, \quad \ell_z, \ell_x \gg 1 \quad (49)$$

such that

$$\gamma \ell_x = O(1).$$

This, of course, is not sufficient to ensure the existence of scaling limit until we specify the strength of  $\mu$ . For monochromatic wave, we set  $\tilde{k} = 1$ .

To study scaling limits with a low Fresnel number it is convenient to use the Wigner distribution

$$W(z, \mathbf{x}, \mathbf{p}) = \frac{1}{(2\pi)^d} \int e^{-i\mathbf{p} \cdot \mathbf{y}} \Psi \left( z, \mathbf{x} + \frac{\gamma \mathbf{y}}{2} \right) \overline{\Psi \left( z, \mathbf{x} - \frac{\gamma \mathbf{y}}{2} \right)} d\mathbf{y} \quad (50)$$

which satisfies a closed-form equation

$$\frac{\partial W}{\partial z} + \mathbf{p} \cdot \nabla W + \sigma \mathcal{L}W = 0, \quad (51)$$

with

$$\mathcal{L}W(z, \mathbf{x}, \mathbf{p}) = i \int e^{i\mathbf{q} \cdot \mathbf{x} \ell_x} [W_z(\mathbf{x}, \mathbf{p} + \ell_x \gamma \mathbf{q}/2) - W_z(\mathbf{x}, \mathbf{p} - \ell_x \gamma \mathbf{q}/2)] \widehat{V}(z \ell_z, d\mathbf{q}). \quad (52)$$

We shall refer to eq. (51) as the Wigner-Moyal equation, the derivation of which is given in Appendix A.

Many useful quantities can be recovered from the Wigner distribution. For instance, it is real and its  $\mathbf{p}$ -integral is the modulus square of the function

$$\int_{\mathbb{R}^d} W(\mathbf{x}, \mathbf{p}) d\mathbf{p} = |\Psi(\mathbf{x})|^2, \quad (53)$$

so we may think of  $W(\mathbf{x}, \mathbf{p})$  as wave number-resolved mass density. Additionally, its  $\mathbf{x}$ -integral is

$$\int_{\mathbb{R}^d} W(\mathbf{x}, \mathbf{p}) d\mathbf{x} = \left(\frac{2\pi}{\gamma}\right)^d |\widehat{\Psi}|^2(\mathbf{p}/\gamma).$$

The energy flux is expressed through  $W(\mathbf{x}, \mathbf{p})$  as

$$\frac{1}{2i} (\Psi \nabla \Psi^* - \Psi^* \nabla \Psi) = \int_{\mathbb{R}^d} \mathbf{p} W(\mathbf{x}, \mathbf{p}) d\mathbf{p} \quad (54)$$

and its second moment in  $\mathbf{p}$  is

$$\int |\mathbf{p}|^2 W(\mathbf{x}, \mathbf{p}) d\mathbf{p} = |\nabla \Psi(\mathbf{x})|^2. \quad (55)$$

Indeed one can recover from the Wigner distribution all but a constant factor, depending only on  $z$ , about the wave amplitude by using this property

$$\int W(z, \mathbf{x}, \mathbf{p}) e^{i\mathbf{p} \cdot \mathbf{y}} d\mathbf{p} = \Psi(z, \mathbf{x} + \frac{\gamma \mathbf{y}}{2}) \Psi^*(z, \mathbf{x} - \frac{\gamma \mathbf{y}}{2})$$

or

$$\Psi(z, \mathbf{x}_1) \Psi^*(z, \mathbf{x}_2) = \int W(z, \frac{1}{2}(\mathbf{x}_1 + \mathbf{x}_2), \mathbf{q}) \exp [i\gamma^{-1} \mathbf{q} \cdot (\mathbf{x}_1 - \mathbf{x}_2)] d\mathbf{q}.$$

By setting  $\mathbf{x}_2 = 0$  we obtain

$$\Psi(z, \mathbf{x}_1) \Psi^*(z, 0) = \int W(z, \frac{1}{2} \mathbf{x}_1, \mathbf{q}) \exp [i\gamma^{-1} \mathbf{q} \cdot \mathbf{x}_1] d\mathbf{q}.$$

The family of self-averaging scaling limits can be divided into two groups depending on whether  $\gamma \ell_x \sim 1$  or  $\gamma \ell_x \rightarrow 0$ . The following formulation of scaling limits provides a different perspective on the convergence results proved in [8].

**Theorem 1** *Let Assumptions 1 and 2 be satisfied. Let  $\gamma \ell_x = 1 > 0$ .*

*As  $\gamma \rightarrow 0, \ell_x, \ell_z, \sigma \rightarrow \infty$  in one of the following ways the Wigner distribution, as weak solution of the Wigner-Moyal equation, converges in probability to the solution of the transport equation*

$$\frac{\partial}{\partial z} W(z, \mathbf{x}, \mathbf{p}) + \mathbf{p} \cdot \nabla W(z, \mathbf{x}, \mathbf{p}) = 2\pi \int K(\mathbf{p}, \mathbf{q}) [W(z, \mathbf{x}, \mathbf{q}) - W(z, \mathbf{x}, \mathbf{p})] d\mathbf{q} \quad (56)$$

where  $K(\mathbf{p}, \mathbf{q})$  is a nonnegative kernel given as follows.

(a) *If  $\sigma \sim \sqrt{\ell_z}, \ell_x \ll \ell_z$  then*

$$K(\mathbf{p}, \mathbf{q}) = \Phi(0, \mathbf{q} - \mathbf{p}) \quad (57)$$

(b) *If  $\sigma \sim \sqrt{\ell_x}, \ell_x \gg \ell_z, d \geq 3$  then*

$$K(\mathbf{p}, \mathbf{q}) = \delta\left(\frac{|\mathbf{q}|^2 - |\mathbf{p}|^2}{2}\right) \left[ \int \Phi(w, \mathbf{q} - \mathbf{p}) dw \right]. \quad (58)$$

(c) *If  $\sigma \sim \sqrt{\ell_z}, \ell_x \sim \ell_z$  then*

$$K(\mathbf{p}, \mathbf{q}) = \Phi\left(\frac{|\mathbf{q}|^2 - |\mathbf{p}|^2}{2}, \mathbf{q} - \mathbf{p}\right). \quad (59)$$

**Theorem 2** *Let Assumptions 1 and 2 be satisfied. Let  $\gamma \ell_x \rightarrow 0$ .*

*As  $\mu \rightarrow \infty$  under the following additional assumption on the scaling parameters the Wigner distribution converges in probability as a generalized function on  $\mathbb{R}^{2d}$  to the solution of the transport equation*

$$\frac{\partial}{\partial z} W(z, \mathbf{x}, \mathbf{p}) + \mathbf{p} \cdot \nabla W(z, \mathbf{x}, \mathbf{p}) = \nabla_{\mathbf{p}} \cdot \mathbf{D} \nabla_{\mathbf{p}} W \quad (60)$$

where  $D$  is a symmetric, nonnegative-definite matrix given as follows.

(a) If  $\sigma \sim (\gamma\ell_x)^{-1}\sqrt{\ell_z}$ ,  $\ell_x \ll \ell_z$  then

$$\mathbf{D} = \pi \int \Phi(0, \mathbf{q}) \mathbf{q} \otimes \mathbf{q} d\mathbf{q}. \quad (61)$$

(b) If  $\sigma \sim (\gamma\ell_x)^{-1}\sqrt{\ell_x}$ ,  $\ell_x \gg \ell_z$ ,  $d \geq 3$  then

$$\mathbf{D}(\mathbf{p}) = \pi |\mathbf{p}|^{-1} \int_{\mathbf{p}, \mathbf{p}_\perp=0} \int \Phi(w, \mathbf{p}_\perp) dw \mathbf{p}_\perp \otimes \mathbf{p}_\perp d\mathbf{p}_\perp. \quad (62)$$

(c) If  $\sigma \sim (\gamma\ell_x)^{-1}\sqrt{\ell_z}$ ,  $\ell_x \sim \ell_z$  then

$$\mathbf{D}(\mathbf{p}) = \pi \int \Phi(\mathbf{p} \cdot \mathbf{q}, \mathbf{q}) \mathbf{q} \otimes \mathbf{q} d\mathbf{q}. \quad (63)$$

Eq. (60) with (61), (62) and (63) are the geometrical optics limit of eq. (56) with (57), (58) and (59), respectively.

The standard radiative transfer scaling is the one that leads to eq. (56) with the kernel (59) [1]. Eq. (56) with (57) is closely related to the mean Wigner distribution in the Gaussian white-noise model [9], while eq. (56) with (58) is closely related to the  $z$ -independent model [25], [7].

Besides the limiting transport equations, the self-averaging aspect is of paramount importance. From the perspective of the quantum stochastic dynamics in a random environment as modeled by the Schrödinger equation with a random potential, self-averaging means that due to the spatial and temporal diversity experienced by the wave function the quantum dynamics has in the scaling limit a classical probabilistic (i.e. jump or diffusion processes in momentum) description which is independent of the particular realization of the environment. The transition from a unitary evolution to an irreversible process is of course the outcome of the phase-space coarse-graining by the test functions. The above results are a rigorous demonstration of decoherence, a mechanism believed to be responsible for the emergence of the classical world from the quantum one [20], [27].

#### 4.3. Exactly solvable models

Among the various scaling limits, two, Eq. (56)(a) and (60)(a), are exactly solvable. To see the dependence on the wave-length, let us set  $\gamma\ell_x = \lambda$  fixed. Then the resulting equation in the regime of Theorem 1(a) can be written as

$$\begin{aligned} \frac{\partial}{\partial z} W(z, \mathbf{x}, \mathbf{p}) + \mathbf{p} \cdot \nabla W(z, \mathbf{x}, \mathbf{p}) \\ = 2\pi\lambda^{-2} \int \Phi(0, \mathbf{q}) [W(z, \mathbf{x}, \mathbf{p} + \lambda\mathbf{q}) - W(z, \mathbf{x}, \mathbf{p})] d\mathbf{q} \end{aligned} \quad (64)$$

whose Green function is given by

$$\begin{aligned} G_W(z, \mathbf{x}, \mathbf{p}; \bar{\mathbf{x}}, \bar{\mathbf{p}}) \\ = \frac{1}{(2\pi)^{2d}} \int e^{i(\mathbf{w} \cdot (\mathbf{x} - \bar{\mathbf{x}}) + \mathbf{r} \cdot (\mathbf{p} - \bar{\mathbf{p}}) - z\mathbf{w} \cdot \bar{\mathbf{p}})} \exp \left[ -1/(2\lambda^2) \int_0^z D_*(\lambda(\mathbf{r} + \mathbf{w}(z-s))) ds \right] d\mathbf{r} d\mathbf{w} \end{aligned} \quad (65)$$

with the wave structure function

$$D_*(\mathbf{x}) = \int \Phi(0, \mathbf{q}) [1 - e^{i\mathbf{x} \cdot \mathbf{q}}] d\mathbf{q}$$

The Green function for (60)(a) can be similarly solved by taking the (partial) inverse Fourier transform in  $\mathbf{p}$ . In the next section we will use the explicit solution given here to analyze the so-called time reversal procedure.

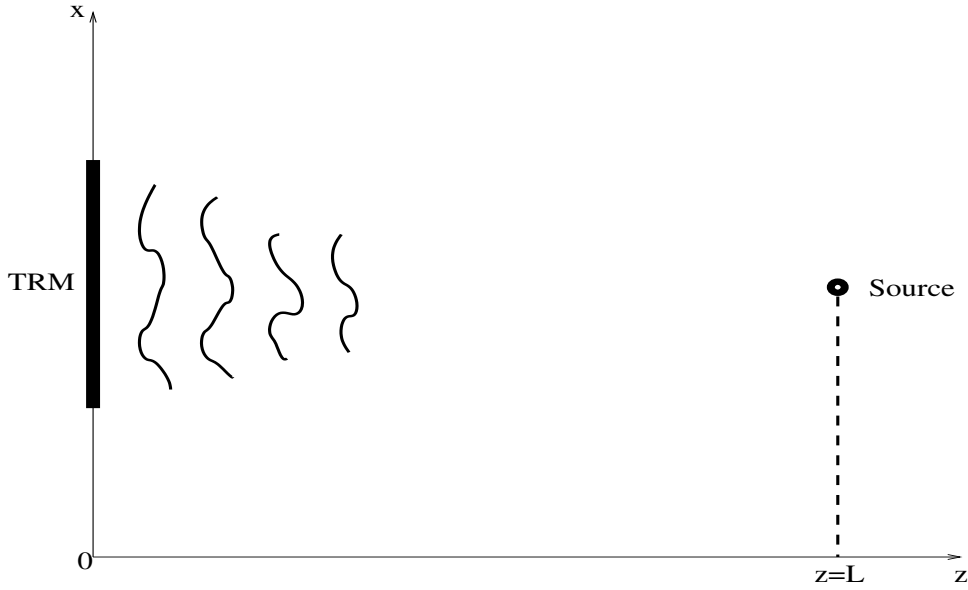


**Figure 2.** The time reversal procedure. A source with central wavelength  $\lambda_0$  emits a pulse. The transmitted field is recorded, stored and time reversed at the mirror of size  $a$  at a distance  $L$  away, and then sent back toward the source point. There it refocuses on the spot size,  $\rho_{\text{tr}}$ , described by (75) when the medium is homogeneous. Medium heterogeneity typically enhances the refocusing resolution.

### 5. Analysis of time reversal with the exactly solvable transport equation

Let us briefly review the time reversal operation and its mathematical formulation. A cartoon of a time reversal experiment is given in Figure 2.

Let the time-reversal array (TRA) be located on the plane  $z = 0$  and the source at the parallel plane a  $L$ -distance away with an aperture  $A$ . The aperture function of the mirror is, in the simplest form, the indicator function  $\mathbb{I}_A$  of the set  $A$  representing the physical boundary of the mirror. Let  $G_H(0, \mathbf{x}, L, \mathbf{y})$  be the Green's function, with the point source located at  $(L, \mathbf{y})$ , for the reduced wave (Helmholtz) equation. By the self-adjointness of the Helmholtz equation,  $G_H$  satisfies the symmetry property

$$G_H(0, \mathbf{x}, L, \mathbf{y}) = G_H(L, \mathbf{y}, 0, \mathbf{x}). \quad (66)$$

By reciprocity the wave field  $\Psi_m$  received at the mirror is given by

$$\begin{aligned} \Psi_m(\mathbf{x}_m) &= \mathbb{I}_A(\mathbf{x}_m) \int G_H(0, \mathbf{x}_m, L, \mathbf{x}_s) \Psi_0(\mathbf{x}_s) d\mathbf{x}_s \\ &= \mathbb{I}_A(\mathbf{x}_m) \int G_H(L, \mathbf{x}_s, 0, \mathbf{x}_m) \Psi_0(\mathbf{x}_s) d\mathbf{x}_s. \end{aligned}$$

In the time-harmonic setting of the present setting, time reversal procedure is equivalent to phase conjugation. After phase conjugation and back-propagation we have at the source plane the wave field

$$\Psi^B(\mathbf{x}) = \int G_H(L, \mathbf{x}, 0, \mathbf{x}_m) \overline{G_H(L, \mathbf{x}_s, 0, \mathbf{x}_m)} \mathbb{I}_A(\mathbf{x}_m) \overline{\Psi_0(\mathbf{x}_s)} d\mathbf{x}_m d\mathbf{x}_s.$$

In the parabolic approximations the Green's function  $G_H(L, \mathbf{x}, 0, \mathbf{y})$  is approximated by  $e^{i\tilde{k}L}G(L, \mathbf{x}, \mathbf{y})$  where  $G(L, \mathbf{x}, \mathbf{y})$  is the propagator of the Schrödinger equation (44). The time-reversed, refocused field then is approximated by

$$\begin{aligned}\Psi^B(\mathbf{x}) &= \int G_S(L, \mathbf{x}, \mathbf{x}_m) \overline{G_S(L, \mathbf{x}_s, \mathbf{x}_m)} \overline{\Psi_0(\mathbf{x}_s)} \mathbb{I}_A(\mathbf{x}_m) d\mathbf{x}_m d\mathbf{x}_s \\ &= \int e^{i\mathbf{p}\cdot(\mathbf{x}-\mathbf{x}_s)/\gamma} W(L, \frac{\mathbf{x}+\mathbf{x}_s}{2}, \mathbf{p}) \overline{\Psi_0(\mathbf{x}_s)} d\mathbf{p} d\mathbf{x}_s\end{aligned}\quad (67)$$

where the Wigner distribution  $W$  is given by

$$\begin{aligned}W(L, \mathbf{x}, \mathbf{p}) & \\ &= \frac{1}{(2\pi)^d} \int e^{-i\mathbf{p}\cdot\mathbf{y}} G_S(L, \mathbf{x} + \gamma\mathbf{y}/2, \mathbf{x}_m) \overline{G_S(L, \mathbf{x} - \gamma\mathbf{y}/2, \mathbf{x}_m)} \mathbb{I}_A(\mathbf{x}_m) d\mathbf{y} d\mathbf{x}_m.\end{aligned}\quad (68)$$

This is a mixed-state type of Wigner distribution which satisfies the same Wigner-Moyal equation (51)-(52), as does the pure-state Wigner distribution (50). The Wigner distribution in (68) has the initial condition

$$W(0, \mathbf{x}, \mathbf{p}) = \frac{\mathbb{I}_A(\mathbf{x})}{\gamma^d (2\pi)^d} \quad (69)$$

which is a  $L^\infty(\mathbb{R}^{2d})$ -function and should be treated as a generalized function on  $\mathbb{R}^{2d}$ . Hence in the regime of Theorem 1(a) we have the expression:

$$W(z, \mathbf{x}, \mathbf{p}) = \frac{1}{\gamma^d (2\pi)^d} \int G_W(z, \mathbf{x}, \mathbf{p}, \bar{\mathbf{x}}, \bar{\mathbf{p}}) \mathbb{I}_A(\bar{\mathbf{x}}) d\bar{\mathbf{x}} d\bar{\mathbf{p}}. \quad (70)$$

Let us now probe the refocused field near a point source located at  $\mathbf{x}_0$ , i.e.  $\Psi_0(\mathbf{x}_s) = \delta(\mathbf{x}_s - \mathbf{x}_0)$ , and write

$$\mathbf{x} = \mathbf{x}_0 + \ell_x^{-1} \mathbf{x}' = \mathbf{x}_0 + \frac{\gamma}{\lambda} \mathbf{x}'.$$

$$\begin{aligned}P_{\text{tr}}(\mathbf{x}_0, \mathbf{x}') &\equiv \Psi^B(\mathbf{x}_0 + \ell_x^{-1} \mathbf{x}') \\ &= \int e^{i\mathbf{p}\cdot\mathbf{x}'/\lambda} W(L, \mathbf{x}_0 + \frac{\gamma\mathbf{x}'}{2}, \mathbf{p}) d\mathbf{p} \\ &= \frac{1}{(2\pi\gamma L)^d} e^{i\frac{\gamma|\mathbf{x}'|^2}{2L\lambda^2}} e^{i\frac{\mathbf{x}'\cdot\mathbf{x}_0}{\lambda L}} \exp\left[-\frac{L}{2\lambda^2} \int_0^1 D_*(s\mathbf{x}') ds\right] \int e^{-i\mathbf{x}'\cdot\bar{\mathbf{x}}/(\lambda L)} \mathbb{I}_A(\bar{\mathbf{x}}) d\bar{\mathbf{x}}\end{aligned}\quad (71)$$

One striking effect of time reversal operation with random media is the statistical stability of the refocal spot, independent of the medium realization from the same ensemble, when the time-reversal aperture is large. In our framework this is readily understood in terms of the self-averaging property of the mixed state Wigner distribution in one of the 6 regimes in Theorem 1 and 2 as  $\ell_x \rightarrow \infty$  which, in the time-reversal setting, is the ratio of the aperture  $a = L_x$  to the correlation length  $L_0$  of the medium.

### 5.1. Anomalous superresolution in time-reversed refocusing

Another somewhat counterintuitive effect in time reversal is that the presence of a strongly scattering medium can greatly *reduce* instead of broadening, the time-reversed focal spot size which can be much smaller than the one in the homogeneous medium. This is called superresolution and has been convincingly explained in the diffusive wave regime by asymptotic

analysis of equation similar to eq. (60) with the diffusion coefficient (63) assuming the spectral density  $\Phi(\mathbf{p} \cdot \mathbf{q}, \mathbf{q})$  is concentrated near  $\mathbf{q} = 0$  in [2].

In what follows, we shall assume the regime of Theorem 1(a) and use the Green function (65) to analyze superresolution in the case of a turbulent medium which after normalization (i.e.  $V$ ) has the power-law spectral density

$$\Phi(\vec{\mathbf{k}}) \sim (1 + |\vec{\mathbf{k}}|^2)^{-H-1/2-d/2} \exp(-|\vec{\mathbf{k}}|^2 \ell_0^2), \quad H \in (0, 1) \quad (72)$$

where  $\ell_0$  is the (normalized) inner scale. We focus on the intermediate (or inertial) regime

$$\ell_0 \ll r = |\mathbf{x}| \ll 1. \quad (73)$$

Calculating the structure function with the power-law spectral density we obtain

$$D_*(r) \approx C_*^2 r^{2H_*}, \quad \text{for } \ell_0 \ll r \ll 1$$

$$H_* = \begin{cases} H + 1/2 & \text{for } H \in (0, 1/2) \\ 1 & \text{for } H \in (1/2, 1] \end{cases}$$

where  $C_* > 0$  is a structure parameter. Substituting it into eq. (71) we obtain the Green function for time-reversal field:

$$P_{\text{tr}}(\mathbf{x}_0, \mathbf{x}) = (L\gamma)^{-d} e^{i\frac{\gamma|\mathbf{x}|^2}{2L\lambda^2}} e^{i\frac{\mathbf{x} \cdot \mathbf{x}_0}{\lambda L}} \hat{\mathbb{I}}_A\left(\frac{|\mathbf{x}|}{\lambda L}\right) T_{\text{tr}}(\mathbf{x}) \quad (74)$$

with

$$T_{\text{tr}}(\mathbf{x}) = \exp\left[-L/(2\lambda^2) \int_0^1 D_*(-s\mathbf{x}) ds\right].$$

Here  $\hat{\mathbb{I}}_A$  is the Fourier transform of the indicator function  $\mathbb{I}_A$  and is related to the Bessel function  $J_1$  when  $A$  is the circular disk of diameter  $a$ .

In the homogeneous medium,  $D_* = 0$  and the refocal spot size is given by the Rayleigh diffraction limit

$$\rho_{\text{tr}} \sim \frac{\lambda L}{a} \quad (75)$$

where  $a$  and  $L$  can both be taken as 1 since they are respectively normalized by  $L_x$  (the back-propagated beam width) and  $L_z$  (the propagation distance).

The effect due to the turbulent medium is described by

$$T_{\text{tr}}(\mathbf{x}) = \exp[-C_*^2 L |\mathbf{x}|^{2H_*} \lambda^{-2}/(4H_* + 2)]$$

which, in the intermediate regime (73), yields a sharper turbulence-induced resolution

$$\begin{aligned} \rho_{\text{tr}} &= \sqrt{\frac{\int |\mathbf{x}|^2 T_{\text{tr}}^2(\mathbf{x}) d\mathbf{x}}{\int T_{\text{tr}}^2(\mathbf{x}) d\xi}} \\ &\sim C_*^{-1/H_*} L^{-1/(2H_*)} \lambda^{1/H_*}, \quad \ell_0 \ll \rho_{\text{tr}} \ll 1 \end{aligned} \quad (76)$$

for  $H_* \in (1/2, 1]$ . That is, the above asymptotic is valid down to the inner scale, the smallest scale of the random medium.

The turbulence-induced resolution (77) is clearly smaller than the diffraction limit (75) when either  $C_*$  is sufficiently large (i.e. sufficiently strong medium fluctuation) or  $H \in (0, 1/2)$  with sufficiently small  $\lambda$  since  $H_* < 1$ . The latter case includes the Kolmogorov spectrum of  $H = 1/3$ .

Finally, if we carry out the same analysis with the Fokker-Planck equation of Theorem 2(a), we obtain that the corresponding refocused field  $\Psi^B(\mathbf{x})$  is Gaussian in the offset variable  $\mathbf{x}$  and the refocal spot size is given by

$$\rho_{\text{tr}} \sim (D_0 L)^{-1/2}.$$

Clearly the refocal spot size in this case is a finite positive constant different from the vanishing  $\lambda$  limit of (76) which is zero. This is due to the singular nature of the limit  $\lambda \rightarrow 0$ .

### 5.2. Uncertainty principle for random media

In this section we note an interesting connection between the forward wave spread and the turbulence-induced resolution in time-reversal.

Let us calculate the energy density in  $\mathbf{x}$

$$|\Psi(z, \mathbf{x})|^2 = \int W(z, \mathbf{x}, \mathbf{p}) d\mathbf{p}$$

with the Gaussian initial wave amplitude  $\exp[-|\mathbf{x}|^2/(2\alpha^2)]$ :

$$\begin{aligned} |\Psi(L, \mathbf{x})|^2 &= \left(\frac{\alpha}{2\sqrt{\pi}}\right)^d \int e^{-|\mathbf{w}|^2[\alpha^2/4 + \lambda^2 L^2/(4\alpha^2)]} \\ &\times \exp\left[-1/(2\lambda^2)L \int_0^1 D_*(\lambda L \mathbf{w} s/\tilde{k}) ds\right] e^{i\mathbf{w}\cdot\mathbf{x}} d\mathbf{w}. \end{aligned}$$

Hence the turbulence-induced broadening can be identified as convolution with the kernel which is the inverse Fourier transform  $\mathcal{F}^{-1}T$  of the transfer function

$$T(\mathbf{x}) = \exp\left[-1/(2\lambda^2)L \int_0^1 D_*(\lambda L \mathbf{x} s) ds\right].$$

We observe that

$$\mathcal{F}^{-1}T(\mathbf{x}) = \frac{1}{\lambda^2 L^2} \mathcal{F}^{-1}T_{\text{tr}}\left(\frac{\mathbf{x}}{\lambda L}\right).$$

We define the turbulence-induced forward spread  $\sigma_*$  as

$$\sigma_* = \sqrt{\int |\mathbf{x}|^2 T^2(\mathbf{x}) d\mathbf{x} / \int T^2(\mathbf{x}) d\mathbf{x}}$$

which together with  $\rho_{\text{tr}}$  then satisfies the uncertainty inequality:

$$\sigma_* \rho_{\text{tr}} \geq \lambda L. \quad (77)$$

The equality holds when  $T_{\text{tr}}$  is Gaussian.

The forward spread is a measure of the enhancement of the effective aperture due to the random medium. This motivates us to define the turbulence-induced aperture as

$$a_* = \frac{\lambda L}{\rho_{\text{tr}}}$$

entirely analogous to (75).

## Acknowledgments

The research is supported in part by U.S. National Science Foundation grant DMS 0306659 and the UC Davis Chancellor's Fellowship.

## Appendix A. Derivation of the Wigner-Moyal equation

Eq. (51) can be formally derived as follows. Differentiating (50) w.r.t.  $z$  and using (44) we have

$$\begin{aligned} \frac{\partial W_z}{\partial z}(\mathbf{x}, \mathbf{p}) &= \frac{1}{(2\pi)^d} \int e^{-i\mathbf{y}\cdot\mathbf{p}} \left[ \frac{i\gamma}{2} \Delta \Psi(z, \mathbf{x} + \frac{\gamma\mathbf{y}}{2}) \Psi^*(z, \mathbf{x} - \frac{\gamma\mathbf{y}}{2}) \right. \\ &\quad \left. - \frac{i\gamma}{2} \Psi(z, \mathbf{x} + \frac{\gamma\mathbf{y}}{2}) \Delta \Psi^*(z, \mathbf{x} - \frac{\gamma\mathbf{y}}{2}) \right] d\mathbf{y} \\ &\quad + \frac{1}{(2\pi)^d} \int e^{-i\mathbf{y}\cdot\mathbf{p}} \left[ \frac{i}{\gamma} V(zl_z, l_x\mathbf{x} + \frac{l_x\gamma\mathbf{y}}{2}) \Psi(z, \mathbf{x} + \frac{\gamma\mathbf{y}}{2}) \Psi^*(z, \mathbf{x} - \frac{\gamma\mathbf{y}}{2}) \right. \\ &\quad \left. - \frac{i}{\gamma} V(zl_z, l_x\mathbf{x} - \frac{l_x\gamma\mathbf{y}}{2}) \Psi(z, \mathbf{x} + \frac{\gamma\mathbf{y}}{2}) \Psi^*(z, \mathbf{x} - \frac{\gamma\mathbf{y}}{2}) \right] d\mathbf{y} \end{aligned}$$

which can be written as

$$\begin{aligned} \frac{\partial W_z}{\partial z}(\mathbf{x}, \mathbf{p}) &= \frac{1}{(2\pi)^d} \int e^{-i\mathbf{y}\cdot\mathbf{p}} \left[ i\nabla_{\mathbf{y}} \cdot \left[ \nabla \Psi(z, \mathbf{x} + \frac{\gamma\mathbf{y}}{2}) \right] \Psi^*(z, \mathbf{x} - \frac{\gamma\mathbf{y}}{2}) \right. \\ &\quad \left. + i\Psi(z, \mathbf{x} + \frac{\gamma\mathbf{y}}{2}) \nabla_{\mathbf{y}} \cdot \left[ \nabla \Psi^*(z, \mathbf{x} - \frac{\gamma\mathbf{y}}{2}) \right] \right] d\mathbf{y} \\ &\quad + \frac{1}{(2\pi)^d} \int e^{-i\mathbf{y}\cdot\mathbf{p}} \left[ i\gamma \int d\hat{V}(zl_z, \mathbf{q}) e^{i\ell_x\mathbf{q}\cdot(\mathbf{x}+\gamma\mathbf{y}/2)} \Psi(z, \mathbf{x} + \frac{\gamma\mathbf{y}}{2}) \Psi^*(z, \mathbf{x} - \frac{\gamma\mathbf{y}}{2}) \right. \\ &\quad \left. - \frac{i}{\gamma} \int d\hat{V}(zl_z, \mathbf{q}) e^{i\ell_x\mathbf{q}\cdot(\mathbf{x}-\mathbf{y}/2)} \Psi(z, \mathbf{x} + \frac{\gamma\mathbf{y}}{2}) \Psi^*(z, \mathbf{x} - \frac{\gamma\mathbf{y}}{2}) \right] d\mathbf{y} \end{aligned}$$

by using the spectral representation. Integrating by parts and expressing the right side in terms of  $W_z$  we obtain eq. (51). Note the cancellation of the term

$$\frac{1}{(2\pi)^d} \int e^{-i\mathbf{y}\cdot\mathbf{p}} \frac{i\gamma}{2} \nabla \Psi(z, \mathbf{x} + \frac{\gamma\mathbf{y}}{2}) \cdot \nabla \Psi^*(z, \mathbf{x} - \frac{\gamma\mathbf{y}}{2}) d\mathbf{y}$$

in the process of integrating by parts.

## References

- [1] G. Bal, G. Papanicolaou and L. Ryzhik: *Self-averaging in time reversal for the parabolic wave equation Stoch. Dynamics* 2, 507-531 (2002).
- [2] P. Blomgren, G. Papanicolaou and H. Zhao: *Super Resolution in Time Reversal Acoustics. J. Acoust. Soc. Am.* 111, 230-248, 2002.
- [3] Bruesselbach, D.C. Jones and D.A. Rockwell and R.C. Lind: *Real-time atmospheric compensation by stimulated Brillouin-scattering phase conjugation. J. Opt. Soc. Am. B* 12, 1434-1447 (1995).
- [4] A. Derode, A. Tourin and M. Fink: *Time reversal versus phase conjugation in a multiple scattering environments. Ultrasonics* 40, 275-280 (2002).
- [5] A. Derode, A. Tourin, J. de Rosny, M. Tanter, S. Yon, and M. Fink, *Taking Advantage of Multiple Scattering to Communicate with Time-Reversal Antennas Phys. Rev. Lett.* 90, 014301 (2003).
- [6] D. Dowling and D. Jackson, *Narrow-band performance of phase-conjugate arrays in dynamic random media, J. Acoust. Soc. Am.*, Vol. 91, 3257-3277, (1992).
- [7] L. Erdős and H.T. Yau, *Linear Boltzmann equation as the weak coupling limit of a random Schrödinger equation, Comm. Pure Appl. Math.* 53, 667-735 (2000).
- [8] A. Fannjiang, *Self-averaging scaling limits for random parabolic waves. Arch. Rat. Mech. Anal*, in press.
- [9] A. Fannjiang, *White-noise and geometrical optics limits of Wigner-Moyal equation for wave beams in turbulent media. Commun. Math. Phys.*, in press.

- [10] A. Fannjiang and K. Solna, *Propagation and Time-reversal of Wave Beams in Atmospheric Turbulence*, *SIAM J. Appl. Math.*, in press.
- [11] M. Fink, *Time-Reversed Acoustics*, *Sci. Am.* 91-97, Nov. (1999)
- [12] M. Fink and J. de Rosny, *Time-reversed acoustics in random media and in chaotic cavities*, *Nonlinearity*15, R1-R18 (2002).
- [13] M. Fink, D. Cassereau, A. Derode, C. Prada, P. Roux, M. Tanter, J.L. Thomas and F. Wu, *Time-reversed acoustics*, *Rep. Progr. Phys.* 63, 1933-1995 (2000).
- [14] M. Fink and C. Prada, *Acoustic time-reversal mirrors*, *Inverse Problems*17, R1-R38 (2001).
- [15] K. Furutsu, *An analytical theory of pulse wave propagation in turbulent media*. *J. Math. Phys.*20 (1979), 617-628.
- [16] J. Gozani, *Pulsed beam propagation through random media*. *Opt. Lett.*21 1996), 1712-1714.
- [17] W. Hodgkiss, H. Song, W. Kuperman, T. Akal, C. Ferla and D. Jackson, *A long-range and variable focus phase-conjugation experiment in a shallow water*, *J. Acoust. Soc. Am.*105, 1597-1604 (1999).
- [18] K. Huang, G. Papanicolaou, K. Solna, C. Tsogka and H. Zhao: *Efficient numerical simulations for long range wave propagation*, preprint.
- [19] A. Ishimaru: *Wave Propagation and Scattering in Random Media*. Academic, New York, 1978.
- [20] E. Joos, H. D. Zeh and I. Stamatescu, *Decoherence and the Appearance of a Classical World in Quantum Theory* (Springer-Verlag, New York, 2003).
- [21] W. A. Kuperman, W.S. Hodgkiss, H.C. Song, T. Akal, C. Ferla and D.R. Jackson, *Phase Conjugation in the Ocean: Experimental Demonstration of an Acoustic Time-Reversal Mirror*, *J. Acoust. Soc. Am.*103(1), 25-40(1997).
- [22] G. Lerosey, J. de Rosny, A. Tourin, A. Derode, G. Montaldo, and M. Fink *Time reversal of electromagnetic waves*, *Phys. Rev. Lett.* 92, 193904 (2004).
- [23] F. Poupaud and A. Vasseur: *Classical and quantum transport in random media*. *Math. Pure et Appli.* 82, 711-748 (2003).
- [24] K.G. Sabra, S.R. Khosla and D.R. Dowling: *Broadband time-reversing array retrofocusing in noisy environments*. *J. Acoust. Soc. Am.*111, 823-830 (2002).
- [25] H. Spohn, *Derivation of the transport equation for electrons moving through random impurities*, *J. Stat. Phys.*, 17, 385-412 (1977).
- [26] M.F. Yanik and S. Fan: *Time reversal of light with linear optics and modulator*. *Phy. Rev. Lett.* 93, 173903 (2004).
- [27] W. H. Zurek, *Decoherence, einselection, and the quantum origins of the classical* *Rev. Mod. Phys.* 75 (2003), 715.